Cesium hydrazinidoborane, the last of the alkali hydrazinidoboranes, studied as potential hydrogen storage material

Carlos Castilla-Martinez, Dominique Granier, Christophe Charmette, Jim Cartier, Pascal Yot, Umit B. Demirci

Cesium hydrazinidoborane, the last of the alkali hydrazinidoboranes, studied as potential hydrogen storage material

Carlos A. Castilla-Martinez,[1] Dominique Granier,[2] Christophe Charmette,[1] Jim Cartier,[1] Pascal G. Yot,[2] Umit B. Demirci [1]*

[1] Institut Européen des Membranes, IEM – UMR 5635, Univ Montpellier, ENSCM, CNRS, Montpellier, France

[2] Institut Charles Gerhardt Montpellier, ICGM – UMR 5253, Univ Montpellier, ENSCM, CNRS, Montpellier, France

* umit.demirci@umontpellier.fr

Abstract

Alkali hydrazinidoboranes $MN_2H_3BH_3$ (M = Li, Na, K, Rb) have been developed for hydrogen storage. To complete the family of $MN_2H_3BH_3$, we focused on cesium hydrazinidoborane $CsN_2H_3BH_3$ (CsHB). It has been synthesized by reaction of cesium with hydrazine borane ($N_2H_4BH_3$) at -20 °C under inert atmosphere, and it has been characterized. A crystalline solid (monoclinic, s.g. $P2_1$ (No. 4)) has been obtained. Its potential for hydrogen storage has been studied by combining different techniques. It was found that, under heating at constant heating rate (5 °C min^{-1}) or at constant temperature (e.g. 120 °C), CsHB decomposes rather than it dehydrogenates. It releases several unwanted gaseous products (e.g. NH_3, B_2H_6) together with H_2, and transforms into a residue that poses safety issues because of shock-sensitivity and reactivity towards O_2/H_2O. Though the destabilization brought by Cs^+ onto the anion $[N_2H_3BH_3]^-$ has been confirmed, the effect is not efficient enough to avoid the aforementioned drawbacks. All of our results are presented herein and discussed within the context of solid-state hydrogen storage.

Keywords

Hydrazine borane; Hydrazinidoborane; Hydrogen storage; Cesium

1. Introduction

Molecular hydrogen H_2 is a renewable, non-toxic and clean fuel that releases water only when it is oxidized (burned). Furthermore, it possesses a high energy density (between 120 and 142 MJ kg^{-1}) that represents more than three times the energy density of gasoline or diesel. It is an excellent alternative to carbonaceous fuels, in fact to fossil fuels [1]. However, the development of an economy of hydrogen as energy carrier (or even as energy source) has shown to be full of obstacles, one of them being storage [2].

Currently, hydrogen can be stored in three ways: (*i*) at high pressure (200-800 bar); (*ii*) in liquid state (at −253 °C) in cryogenic tanks; and, (*iii*) in a material [3]. The most mature technology is the first one, but the most attractive method, and surely the most promising in the near future, is the last one. Two types of materials have to be distinguished: porous materials (e.g. carbon nanotubes, metal organic frameworks, covalent organic frameworks, polymers) adsorbing and desorbing reversibly H_2 at subzero temperatures (generally at −196 °C), and hydrides where H is chemically bonded to an element like magnesium, nickel, boron, and/or nitrogen [4]. Belonging to the second type of materials, boron- and nitrogen-containing compounds have received considerable attention owing to several advantageous features: they have high hydrogen densities (e.g. 19.5 wt. % H for ammonia borane NH_3BH_3); they carry hydridic and protic hydrogens ($H^{\delta-}$ and $H^{\delta+}$) through B−H and N−H bonds, rationalizing the solid state of these compounds at ambient conditions and favoring the H_2 release at mild conditions (e.g. onset temperature of dehydrogenations between 50 and 100 °C); and, they are generally easy and safe to handle when kept under inert atmosphere [5].

An example of boron- and nitrogen-containing compounds is hydrazine borane $N_2H_4BH_3$ (HB). It possesses a high gravimetric hydrogen density with 15.4 wt. % H, and it is stable at room temperature under inert atmosphere [6]. However, neat HB has shown to be unsuitable as hydrogen storage material because it decomposes under heating while producing undesired gaseous by-products (e.g. ammonia NH_3, diborane B_2H_6, and hydrazine N_2H_4) and it generates a shock-sensitive solid product when it is heated above 300 °C [7]. Despite these, HB, which has three $H^{\delta-}$ versus four $H^{\delta+}$, has been considered as precursor of derivatives carrying as much $H^{\delta-}$

as $H^{\delta+}$, thereby alkali hydrazinidoboranes $MN_2H_3BH_3$ have been obtained by chemically modifying HB, namely by substituting one of the $H^{\delta+}$ of the middle N atom of $NH_2NH_2BH_3$ by a metal cation M^+.

The first alkali hydrazinidoborane that was reported is lithium hydrazinidoborane $LiN_2H_3BH_3$ (LiHB; 11.7 wt. % H):

$$MH\ (s) + NH_2NH_2BH_3\ (s) \rightarrow NH_2NH(M)BH_3\ (s) + H_2\ (g) \tag{1}$$
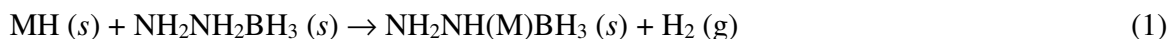
with M = Li and Na. LiHB presents two crystalline phases. The high temperature phase, denoted α-LiHB (monoclinic, s.g. $P2_1/c$), was first reported by Wu et al. [8]. The low temperature phase, β-LiHB (orthorhombic, s.g. $Pbca$), was afterwards found by Moury et al. [9]. Under heating, β-LiHB transforms into α-LiHB that releases 2.6 equiv H_2 and traces of NH_3 below 150 °C. Sodium hydrazinidoborane $NaN_2H_3BH_3$ (NaHB; 8.9 wt. % H) was synthesized (Eq. 1) by Moury et al. by mechanosynthesis at ca. −30 °C [10]. The product obtained is a crystalline solid (monoclinic, s.g. $P2_1/n$) that starts the dehydrogenation process at ca. 60 °C, releasing H_2 with traces of NH_3 and N_2. Potassium hydrazinidoborane $KN_2H_3BH_3$ (KHB; 7.2 wt. % H; monoclinic, s.g. $P2_1$) was synthesized by Chua et al., in a stainless steel reactor containing dissolved HB because of the high reactivity of KH towards HB [11]:

$$KH\ (s) + NH_2NH_2BH_3\ (sol) \rightarrow NH_2NH(K)BH_3\ (s) + H_2\ (g) \tag{2}$$

It is the least stable of these hydrazinidoboranes as it is able to release H_2 from ca. 50 °C. Recently, we reported rubidium hydrazinidoborane $RbN_2H_3BH_3$ (RbHB, 4.6 wt. % H; monoclinic, s.g. $P2_1$) [12]. It was synthesized by reaction of metallic rubidium and HB dissolved in THF:

$$Rb\ (s) + NH_2NH_2BH_3\ (sol) \rightarrow NH_2NH(Rb)BH_3\ (s) + ½\ H_2\ (g) \tag{3}$$

It has better dehydrogenation properties than the parent HB and comparable to the ones of LiHB. Unlike the aforementioned hydrazinidoboranes, RbHB is not stable when stored at room temperature and under argon atmosphere; it decomposes liberating H_2 and forming boron- and nitrogen-containing polymeric compounds.

Cesium hydrazinidoborane (CsHB; 3.4 wt. % H) is the last derivative of the series. We focused on this derivative also, because it is essential to better understand boron and nitrogen-containing compounds through the discovery of new materials. Our other objectives were as follows:

3

widening the prospects for the hydrogen storage application; and, opening up new opportunities. CsHB was synthesized by making metallic Cs react with HB in solution, under argon atmosphere:

$$Cs\ (s) + NH_2NH_2BH_3\ (sol) \rightarrow NH_2NH(Cs)BH_3\ (s) + \frac{1}{2}\ H_2\ (g) \tag{4}$$
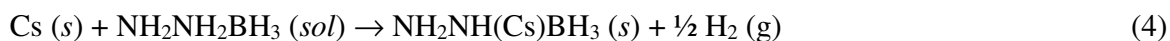
A crystalline material was recovered, characterized, and studied while focusing on its potential as hydrogen storage material. Herein CsHB is thus presented for the first time.

2. Material and methods

The experiments described hereafter were carried out in an inert atmosphere of argon, either in a glove box (MBraun M200B; $O_2 < 0.1$ ppm and $H_2O < 0.1$ ppm) or using a vacuum-argon line. HB was synthesized according to a procedure we previously developed [7]. Typically, 21.59 g of hydrazine hemisulfate $N_2H_4 \cdot \frac{1}{2}H_2SO_4$ ($\geq$ 98%, Sigma-Aldrich) and 10.12 g of sodium borohydride $NaBH_4$ ($\geq$ 98%, Sigma-Aldrich) were weighted in the glove box. They were suspended, under stirring, in 150 mL of anhydrous 1,4-dioxane ($\geq$ 99.8%, Sigma-Aldrich) in a round-bottom flask. The reaction was performed at 30°C for 48 h. After this time, the suspension (i.e. $NaSO_4$) was filtered, and a solution (HB dissolved in 1,4-dioxane) was recovered. The solvent was removed under vacuum and HB was obtained (yield of 80%, and purity of 99.6%).

As it is the case with Rb [12], HB readily reacts with metallic cesium. We therefore attempted to synthesize CsHB at subzero conditions, here at −20 °C; for this, a coolant and a cooling jacket were used. Under inert atmosphere, 120 mg of HB was dissolved in 20 mL of extra dry THF (99.5%, Acros Organics), and 300 mg of Cs (ingot, $\geq$ 99.95%, Sigma-Aldrich) was weighted and put into a round bottom flask inside the argon-filled glove box. The flasks were transferred outside the glove box. The Cs-containing flask was immersed in the cooling bath and the HB solution was cooled down in a freezer. Once the temperature of the flasks was stabilized, the HB solution was poured into the Cs-containing flask, and the reaction was left under stirring for 6 h. After this time, the solid precipitate was washed two times with THF. It was dried for 24 h under vacuum, the remaining Cs was removed, and the solid product CsHB was recovered. In doing so, 340 mg of CsHB was recovered (yield of 85% with respect to Cs).

The molecular structure of CsHB was analyzed by solid-state [11]B magic angle spinning nuclear magnetic resonance (MAS NMR; Varian VNMR4000, 128.31 MHz; using zirconia rotors with a diameter of 3.2 mm), and Fourier Transformed Infrared (FTIR) spectroscopy (NEXUS instrument, ThermoFisher Scientific, equipped with an attenuated total reflection accessory from 600 to 4000 cm^{-1} wavelength). The FTIR analyses were performed under air, but the sample was kept under argon atmosphere in a vial until the last moment before the analysis.

Powder X-ray diffraction (PXRD) analysis was done in a PANalytical X'Pert Pro Multipurpose diffractometer equipped with an X'Celerator detector and using a Bragg Brentano θ-θ reflection geometry with Ni filtered Cu-K$_{\alpha1/\alpha2}$ radiation (λ = 1.5418 Å). The pattern was collected on a spinning glass sample holder protected with Parafilm®¸ and loaded into the glovebox to prevent any contact with O_2 and H_2O. The diffraction pattern was recorded in the 10-80° angle range in 2θ using a step size of 0.017, with a scan step time of ~450 seconds at room temperature. The indexation of the as-collected PRXD pattern was done by using the FoX software [13]. The refinement (Rietveld method) was carried out in the JANA2006 package, and the determination of the position of the Cs atoms was done with the 'SuperFlip' algorithm included in the software [14]. After this, FoX was used to reach the position of the [$N_2H_3BH_3$]$^-$ anions. The Rietveld refinement of the pattern was carried out using a Pseudo-Voight peak shape. The peaks asymmetry was corrected using Howard model (Boole's rule) and preferred orientation using March-Dollase model following (010) direction. The B−H and N−H distances were constrained to 1.20 and 1.04 Å respectively in accordance with the optimization realized by FoX program. The uncertainties of the atomic coordinates for H atoms are not reported here because they were not freely refined. The isotropic thermal parameters (Uiso) were constrained to be identical for all atom types (Uiso = 0.0477(9) Å^2 for the Cs, B, and N atoms; Uiso = 1.2 Å^2 for the H atoms). The locations of the H atoms linked to the N and B atoms were determined by performing a geometry constrained optimization of the structure (Cs, B and N atoms fixed in their initial position) at the force-field level. The atoms of the system were represented as Lennard-Jones charged sites with LJ parameters taken from the UFF force field while the charges were calculated using the QeQ method.

The thermal stability of CsHB was analyzed by thermogravimetric (TG) analysis. A TG analyzer (Netzsch STA 449 F1 Jupiter) coupled to a mass spectrometer (MS; Netzsch QMS 403 D Aëolos Quadro) was used. Differential scanning calorimetry (DSC) analysis (SDT Q600, TA Instruments) was also carried out. For both techniques, the samples preparation was done inside the glovebox, where the powder was enclosed in a Tzero hermetic aluminum crucible to protect it from air. The crucible was pierced with a needle right before the analysis to let release the evolving gases.

The thermal stability of CsHB was besides analyzed at isothermal conditions (90, 100, 110 and 120°C). Typically, 100 mg of CsHB was weighted in the glovebox, placed in a vial and put inside a stainless steel reactor. The reactor was connected to a pressure controller and immersed in an oil bath at the required temperature. The decomposition of CsHB was monitored by the change of pressure inside the reactor. Upon the completion of the reaction, the equivalents of gas (considered as ideal) liberated were calculated and plotted as a function of time. The gases released at these conditions were analyzed by a gas chromatograph (GC; PerkinElmer Clarus 400 equipped with a ShinCarbon ST column) coupled to a mass spectrometer (MS; PerkinElmer Clarus 600 T). The ShinCarbon ST column contains a treated carbon that allows the separation of hydrogen from the gas mixture, with the gas mixture being besides ionized by an electron beam in order to obtain the mass spectrum. Typically, after the reaction had finished and the reactor was cooled down at room temperature, the atmosphere of the reactor was collected with the help of a glass syringe and the sampled gases were injected into the GC column.

3.   Results and discussion

3.1.   Safety issues

All necessary precautions must be taken to work with Cs, CsHB, and the thermolytic solid residues. (*i*) Cs is highly reactive and violently reacts with water. (*ii*) HB must be dissolved in THF before putting into contact with Cs, which allows dissipating the heat released during the exothermic reaction between Cs and HB. This issue is comparable to what we noticed while working with RbHB [12]. (*iii*) CsHB readily reacts with protic solvents like water, ethanol and methanol (occurrence of solvolysis with release of H_2). (*iv*) CsHB has to be stored under inert

atmosphere (preferably, inside a glove box). (*v*) Upon decomposition of CsHB, shock-sensitive products may form. This happened for a sample heated at 100°C. (*vi*) The solid residues forming upon decomposition of CsHB were found to ignite when put under air. Objectively, these cannot be seen as arguments in support of CsHB as hydrogen storage material.

To work under the best conditions of safety, the residues of CsHB must be always kept under inert atmosphere. To dispose of such unstable materials, the recommendation is to: put a small quantity (<100 mg) of the residue in a closed vial; add some mineral oil; slowly add isopropanol (few milliliters dropwise) to neutralize the sample by solvolysis (resulting in H_2 release and formation of borates); repeat the process with a more reactive solvent like methanol; and, repeat with water. The as-obtained borates (basic compounds) can be finally and safely trashed with the aqueous bases.

3.2. *Molecular structure of CsHB*

CsHB is a white fine powder. It is insoluble in anhydrous organic solvents like dioxane, toluene, THF or dimethyl carbonate. Solubility in water, methanol and ethanol could not be assessed as CsHB readily reacts with these protic solvents (occurrence of hydrolysis or alcoholysis with release of H_2). Molecular analyses based on solutions have thus been discarded.

CsHB was analyzed by FTIR, and the resulting spectrum was compared to the one of HB (Figure 1). The N−H stretching bands (3500-2600 cm^{-1}) of CsHB are less complex. This indicates a weaker interaction between the $H^{\delta+}$ of the N_2H_3 group and the $H^{\delta-}$ of the BH_3 moiety, and thus a lesser stability in comparison to HB. The bands due to the B−N and BN−N bonds are more intense for CsHB, suggesting shorter bonds. For the B−H region, CsHB displays the bands at a lower wavelength than HB does. These observations are all due to the insertion of Cs^+, which modifies the chemical environment and the electronic properties of the molecular entity $[N_2H_3BH_3]^-$ [15-17]. It is worth mentioning that the spectrum of CsHB is much comparable to the spectral fingerprint of the sister compound RbHB [12].
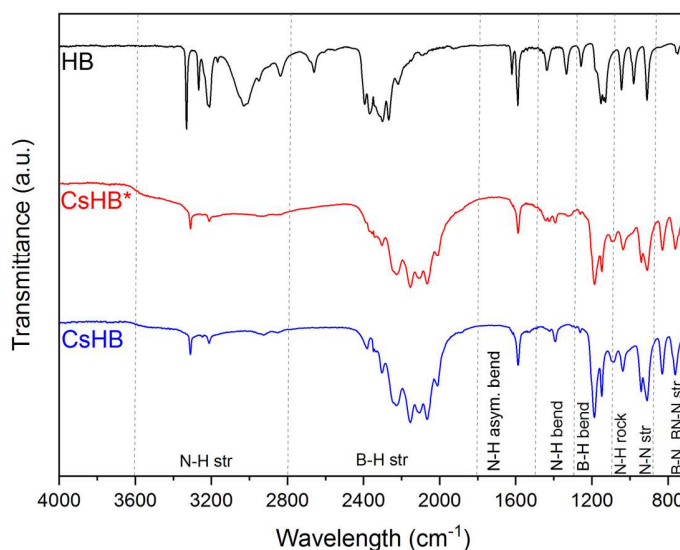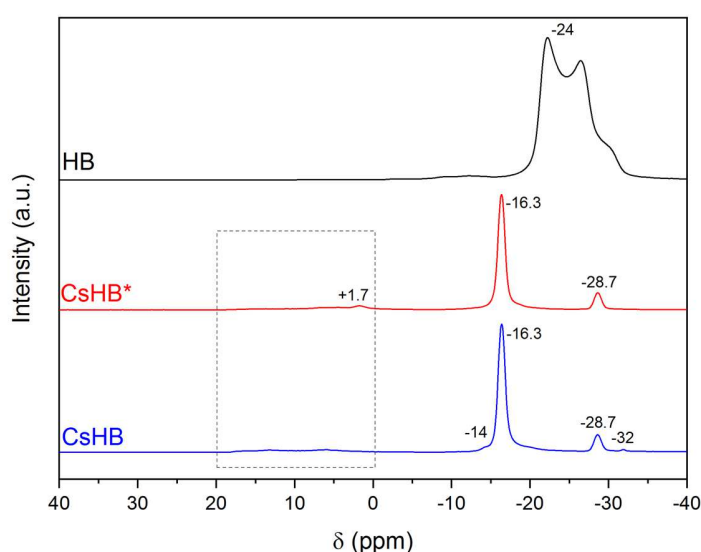
Figure 1. FTIR spectra of CsHB, CsHB after two months (i.e. aged CsHB denoted CsHB*), and HB. The bands are assigned.

CsHB was analyzed by ^{11}B MAS NMR (Figures 2 and S1). The spectrum is different from that of HB, and typical of an alkali derivative [8-12]. CsHB presents a Gaussian-like signal at −16.3 ppm (versus a double-horn signal shape due to quadrupolar coupling [18], signal centered at −24 ppm for HB), which is ascribed to its NBH$_3$ environment. The change in the signal shape indicates a more isotropic environment around the B atom favored by the presence of Cs$^+$. At least five other signals, of lower intensity, can be seen and have been tentatively assigned [19-22]. Three of them are at negative chemical shifts. The signals at −32 and −14 ppm are attributed to BH$_4$ and BH$_2$ environments respectively. The concomitance of the BH$_4$ and BH$_2$ suggests the possible formation of a dimeric compound, tentatively that of [CsN$_2$H$_3$BH$_2$CsN$_2$H$_3$]$^+$[BH$_4$]$^−$ [23]. The signal at −28.7 ppm is untypical of a BH$_3$ environment. It is likely due to a boron hydride with B−B bonds (boron clusters) such as the anion B$_3$H$_8^−$. Such an attribution is consistent with the chemical shift of −29.8 ppm reported elsewhere for CsB$_3$H$_8$ [24] and with the formation of this salt [25,26]. The following reaction might be suggested based on the findings reported in refs. [25,26]:

$$\text{Cs } (s) + 3 \text{ BH}_3 \ (sol) \rightarrow \text{CsB}_3\text{H}_8 \ (s) + \tfrac{1}{2} \text{ H}_2 \ (g) \tag{5}$$
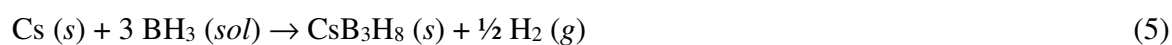
where BH$_3$ would directly come from HB or from in situ forming B$_2$H$_6$ by decomposition of HB (as shown below B$_2$H$_6$ formed as by-product in our conditions). The other signals shown by CsHB are at positive chemical shifts and they are ascribed to BN$_3$, and BN$_2$H environments. They suggest that slight evolution of CsHB, or of its possible dimer, into a polyborazylene-like compound [19] is likely to occur during synthesis, storage of the sample, and/or fast rotation of the sample during NMR analysis.

Figure 2. ^{11}B MAS NMR spectra of CsHB, CsHB after two months (i.e. aged CsHB denoted CsHB*), and HB. The chemical shifts in ppm of the signals are indicated. The dashed line box focuses on the signals of very low intensity at positive chemical shift; cf. Figures S1 and S2 for zoomed versions of the spectra.

3.3. Stability of CsHB under inert atmosphere

After its synthesis, CsHB was stored for two months inside the glovebox to be further analyzed by FTIR and ^{11}B MAS NMR. The FTIR analysis shows that CsHB and aged CsHB (denoted CsHB*) present almost identical bands (Figure 1). For the latter, however, there is a slight broadening of the N−H stretching and bending regions. This could be due to the formation of a small amount of additional polymeric species.

The ^{11}B MAS NMR spectra of CsHB and CsHB* do not present significant differences (Figures 2 and S2). The BH$_3$ environment at −16.3 ppm is the main peak in both spectra, showing the

stability of CsHB. The signals at −32 and −14 ppm have disappeared for CsHB*. The spectrum of CsHB* shows an additional signal at +1.7 ppm. It can be due to a BN$_4$ environment [22]. These last two observations suggest a slight evolution of the sample, likely of the species [CsN$_2$H$_3$BH$_2$CsN$_2$H$_3$]$^+$[BH$_4$]$^−$.

Based on these ^{11}B MAS NMR and FTIR analyses, it may be concluded that CsHB is rather stable when kept at ambient temperature under argon atmosphere. It is however less stable than HB, which is stable in the solid state [7]. This suggests that the size of a big cation like Cs$^+$ has an important effect of destabilization on the [NH$_2$NBH$_3$]$^−$ anion. To avoid the evolution of CsHB, the compound can be stored at low temperature (subzero conditions). However, as mentioned before, there are safety issues in storing CsHB in an ambient where moisture is present. A water-tight container must be used, carefully closed and stored in a freezer. CsHB is more stable than RbHB when they are kept at ambient temperature under argon atmosphere. The latter compound was found to significantly dehydropolymerize [12]. RbHB is in fact synthesized at room temperature. In such conditions, the exothermic reaction between HB and Rb may lead to the formation of (unidentified) side-products that are instable and that react over time.

3.4. Crystal structure of CsHB

CsHB was analyzed by PXRD (Figure 3). The pattern was compared to that of HB, and the presence of a new phase was confirmed. The omitted Bragg peaks during the structure refinement were identified as coming from the Parafilm® film used to protect the solid.

The PXRD pattern of CsHB (Figure 3) was indexed and refined as described previously. The position of the Cs atoms and that of the [N$_2$H$_3$BH$_3$]$^−$ anions were determined. In doing so, the crystallographic parameters of CsHB (Table 1) as well as the experimental structural parameters (Table S1) were compiled, and the calculated pattern was found to be in good fit with the experimental one (Figure S3).

CsHB was successfully indexed as a single phase in a monoclinic $P2_1$ (No. 4) unit cell (Figure 4), with Z = 2, a = 5.9156(5) Å, b = 7.0091(5) Å, c = 6.0023(5) Å, and β = 108.389(4)° (Table 1). Except for β-LiHB (orthorhombic, s.g. *Pbca*) [9], all of the other hydrazinidoboranes crystallize

in a monoclinic unit cell. α-LiHB does in a space group $P2_1/c$ [8] while NaHB does in a space group $P2_1/n$ [10]. CsHB is isostructural with KHB [11] and RbHB [12].
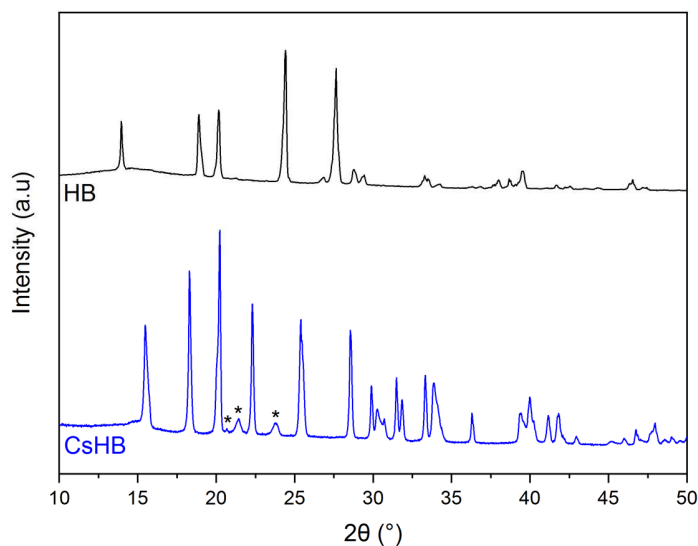
**Figure 3.** PXRD patterns of CsHB and HB. The peaks indicated by the symbol * belong to Parafilm® foil.

Table 1. Crystallographic parameters of CsHB.

Formula	$CsN_2H_3BH_3$
Unit cell	Monoclinic
s.g.	$P2_1$ (No. 4)
Z	2
***a* (Å)**	5.9156(5)
***b* (Å)**	7.0091(5)
***c* (Å)**	6.0023(5)
***β* (°)**	108.389(4)
***V* (Å^3)**	236.16(3)
Density	2.5
Temperature	20 °C
$R_{(all)}/wR_{(all)}$	7.32/9.03
$R_{(obs)} / wR_{(obs)}$	7.32/9.03
GoF	5.08
Rp	6.66
wRp	10.17

In comparison with HB [7], CsHB has a bigger unit cell volume per formula (V/Z = 80.153 versus 118.083 Å^3). This is due to the big size of the cation Cs$^+$. If CsHB is compared to its amidoborane analogous, i.e. cesium amidoborane (CsAB; orthorhombic, s.g. *Pnam*) [27], it has a

11

bigger unit cell volume per formula (V/Z = 99.42 versus 118.083 Å^3). This is in good agreement with the bigger size of the $[N_2H_3BH_3]^-$ anion of CsHB.

The coordination sphere of Cs^+ is featured by six surrounding $[N_2H_3BH_3]^-$ entities (Figure S4). The other hydrazinidoboranes have coordination numbers of four (LiHB) [8,9], five (NaHB) [10], four (KHB) [11], and six (RbHB) [12]. RbHB and CsHB can coordinate more anions due to the bigger size of the cation. In comparison with the amidoboranes, CsAB is surrounded by seven $[NH_2BH_3]^-$ anions [27], which is consistent with the smaller size of these anions (versus the $[N_2H_3BH_3]^-$ anions in CsHB).
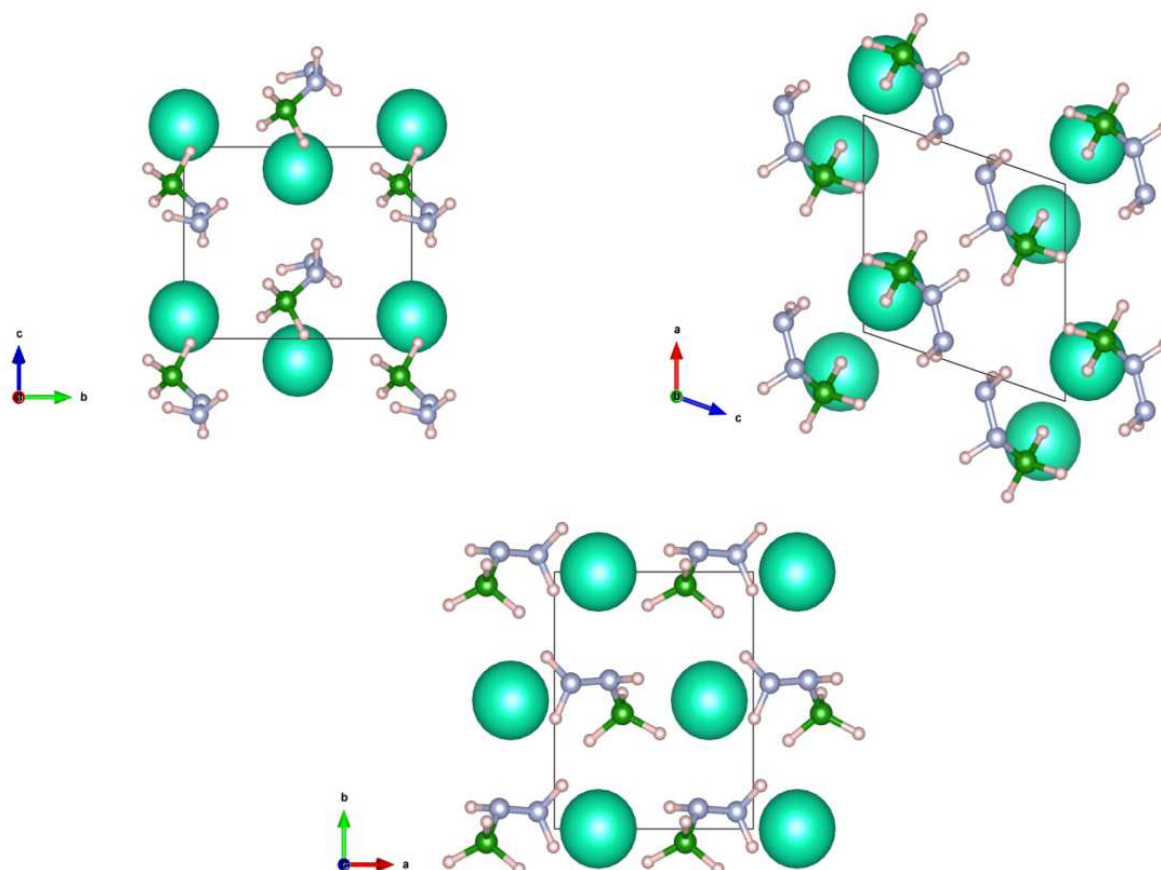

Figure 4. Crystal structure of CsHB along the [100], [010] and [001] directions. The H, B, N and Cs atoms are represented by pink, green, blue and turquoise spheres, respectively.

The positions of the H atoms were obtained by computational methods, allowing us to determine the interatomic distances (Figure S5). The shortest interatomic Cs⋯Cs distance is 4.326(4) Å. The shortest Cs−N bond is 3.22(7) Å. Compared to the other hydrazinidoboranes, the M−N distance (M = Li, Na, K, Rb, Cs) shortens as the size of the alkali cation decreases: a bond distance of 3.13 Å was found for RbHB [12], 2.96 Å for KHB [11], 2.41 Å for NaHB [10], and 2.11 Å for LiHB [9]. It is likely that the bond M−N has a higher ionicity for CsHB. The higher ionicity means that more electrons are attracted by the N atom from the Cs^+ cation in comparison with the $H^{\delta+}$ atom of HB; the Lewis basicity of the N atom and that of the $H^{\delta-}$ in the B atom are increased, meaning a higher reactivity of CsHB in comparison with the other alkali hydrazinidoboranes and HB [11,28]. This represents an advantage of the Cs^+ cation over the $H^{\delta+}$ element in terms of destabilization. The B−N bond is shorter for CsHB (1.40(8) Å) in comparison with HB (1.59 Å) [8], which is consistent with the changes observed in the ^{11}B MAS NMR and FTIR analyses.

3.5. *Thermal analyses of CsHB*

The thermal stability of CsHB was followed by TG analysis (heating rate of 5 °C min^{-1}) and the evolving gaseous products were identified by MS (Figure 5). As shown by the DSC curve, there is a first event peaking at 56°C that is endothermic. A similar endothermic event was also observed for HB [7], NaHB [10], KHB [11] and RbHB [12]. They are associated to melting. CsHB starts to decompose at ca. 75 °C, according a complex path as suggested by the DSC and MS results. The decomposition is featured by successive exothermic events. In the range 75-160 °C, CsHB loses 3.5 wt. % of its initial weight. H_2 as main gaseous product, but also NH_3 and B_2H_6, were detected. A second mass loss of ca. 1.4 wt. % occurs in the range of 160-190 °C. There is a third one of ca. 2 wt % above 190 °C. The total weight loss between 75 and 250 °C is 6.9 wt. %. This is twice the 3.4 wt. % H carried by CsHB. This excess of weight loss is due to the release of NH_3 and B_2H_6. The Li, Na and K hydrazinidoboranes release purer H_2 [8-11]. RbHB [12] and CsHB tend to release more unwanted by-products. Big cations are thus less efficient in hindering decomposition of $[N_2H_3BH_3]^-$, in other words, in being selective towards dehydrogenation of the anions $[N_2H_3BH_3]^-$ by dehydropolymerization.
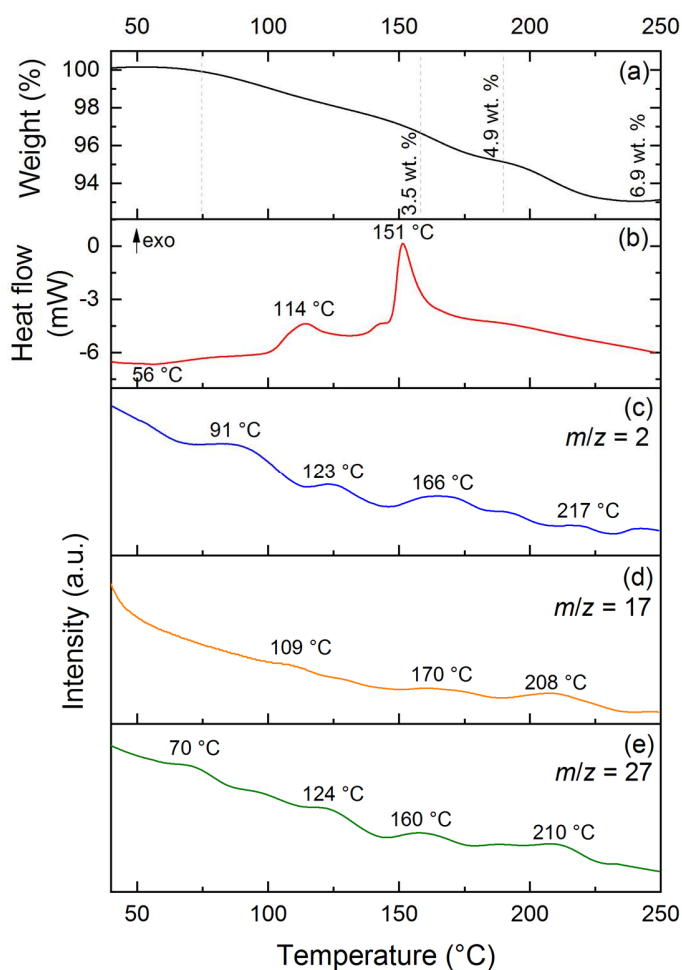
Figure 5. Thermal analysis of CsHB: (a) TG analysis (5 °C min⁻¹); (b) DSC analysis (5 °C min⁻¹); (c,d,e) MS results with m/z = 2, 17, and 27 respectively). Weight losses at 160, 190 and 250 °C, and most of the peak temperatures (°C) are given.

3.6. Decomposition of CsHB in isothermal conditions

The thermal stability of CsHB was besides investigated by heating it at constant temperature, i.e. 90, 100, 110 and 120 °C (Figure 6). In these isothermal conditions, the decomposition of CsHB presents a two-step process preceded by an induction period that becomes shorter as the temperature increases. After the induction period, the sample starts to decompose slowly. This step is short, particularly at 110 and 120 °C (10 and 9 min respectively). It is then followed by a second step of decomposition, which is more important and much faster. This is typically the case at 120°C: the induction period, the first step and the second step are as short as 9, 2 and <1 min

(versus e.g. 25, 10 and >30 min at 90 °C). Note that such a decomposition profile seems to be typical of hydrazinidoboranes; a similar behavior was reported for e.g. NaHB [10] and RbHB [12].
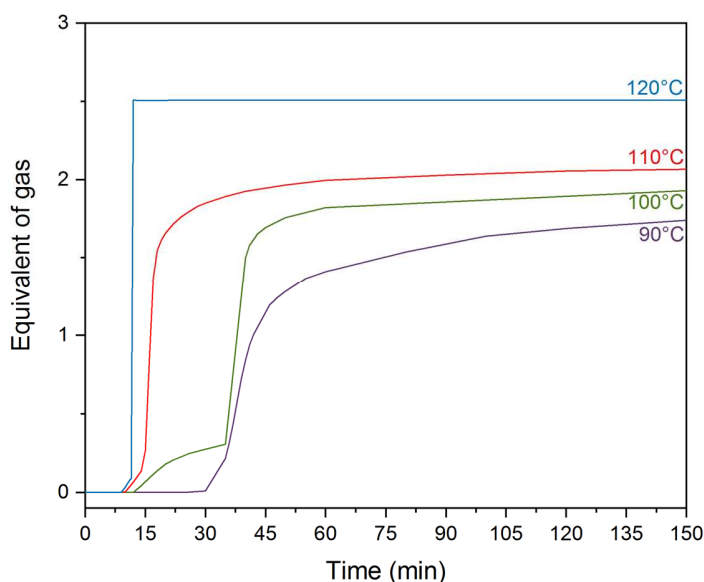

Figure 6. Time evolution of H_2 release from CsHB under heating at isothermal conditions.

The gases produced during these isothermal experiments were analyzed by GC and MS (Figures S6 to S8). As expected, H_2 was detected. However, several unwanted gaseous by-products were also detected: namely, NH_3, B_2H_6 and N_2H_4. With respect to the first two gases, the results are consistent with the TG-MS results. N_2H_4 was not observed by TG-MS but its formation cannot be discarded as, based on our experience, N_2H_4 is able to condensate on cold surfaces (between the TG and MS apparatuses), being thereby not seen by MS [7,9,11].

Tentative reaction paths are proposed to explain the formation of the aforementioned unwanted products (Figure 7). As it has been reported, diammoniate of diborane (DADB) is an intermediate in the decomposition of ammonia borane [29,30]. Evidence of analogues compounds for alkali amidoboranes have also been reported [31]. The formation of ammonia is explained by the formation of an analogous compound of DADB applied to CsHB (Figure 7a). The intermediate $[(NH_2CsNH)_2BH_2]^+[BH_4]^-$ would form, and then, one of the $H^{\delta+}$ atoms would migrate to the end

N atom (i.e. NH_2 group), breaking the N–N bond and resulting in the release NH_3 and H_2 [32]. One of the possible paths to form B_2H_6 is as follows (Figure 7b): it is assumed that the same DADB analogous compound, i.e. $[(NH_2CsNH)_2BH_2]^+[BH_4]^-$, forms. The $[BH_4]^-$ anion would react with another $[BH_4]^-$ anion to liberate B_2H_6 and H_2, with the subsequent growing of the polymer chain by dehydrocoupling. Such mechanisms could explain also the species detected in the TG-MS experiments. The exothermic processes seen in the DSC profile (Figure 5) can be due to the release of NH_3 and H_2, as these processes are known to be exothermic.
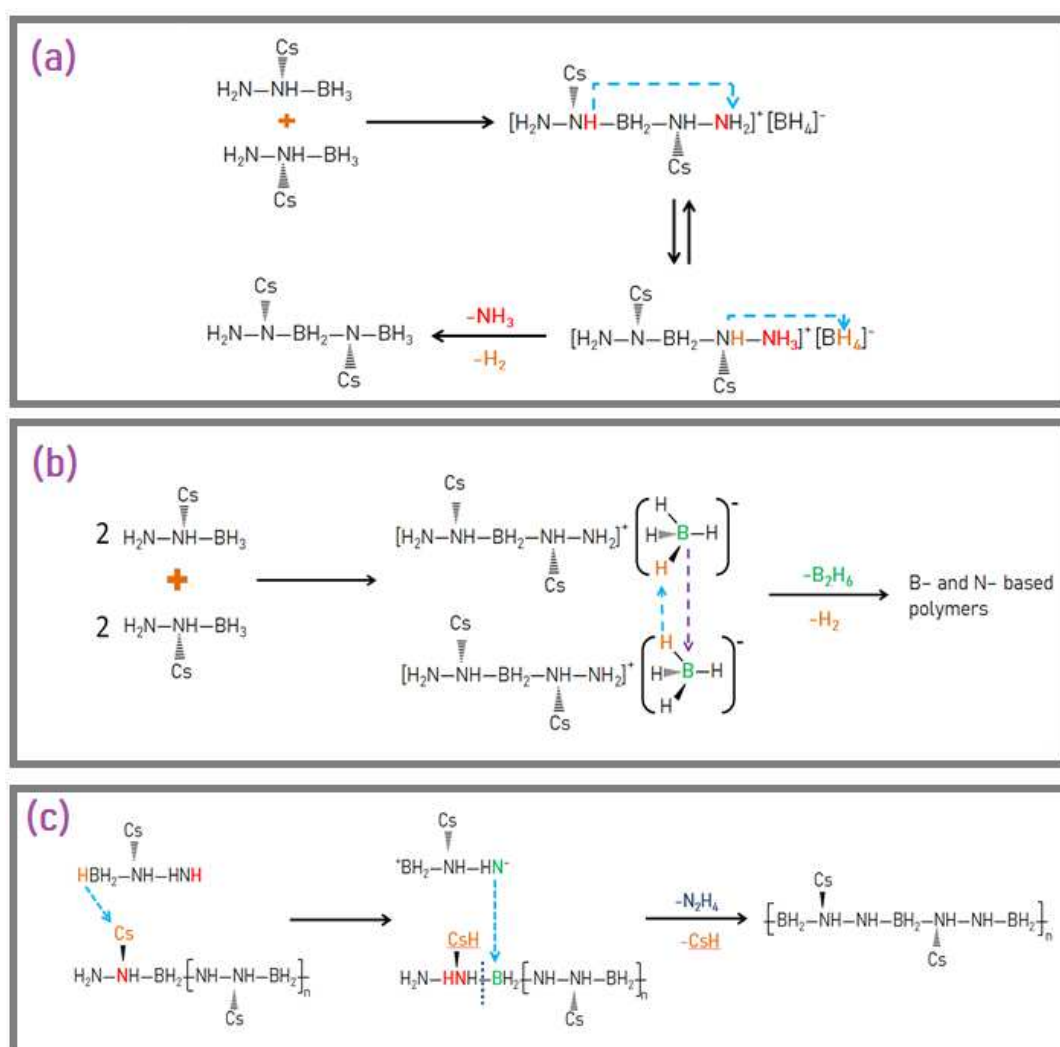
Figure 7. (a) Reaction between 2 molecules of CsHB releasing NH_3 and H_2, resulting in compounds with sp^2 and sp^3 B centers. (b) CsHB molecules forming the intermediate $[(CsN_2H_3)_2BH_2]^+[BH_4]^-$, and then releasing B_2H_6 and H_2, leading to the formation of B- and N-based polymers. (c) Reaction of a polymer chain product of the thermolysis of CsHB and a molecule of CsHB, and this leads to a continued growth of the chain, forming CsH and releasing N_2H_4.

The solid residues recovered after decomposition of CsHB could not be safely handled to analyze them by FTIR and PXRD (cf. sub-section 3.1 for more details about the safety issues). However, we were able to analyze them by ^{11}B MAS NMR. The NMR rotors were indeed filled in the glove box and thereby the samples were protected from air and moisture.

The solid residues that formed after the heat treatments performed at isothermal conditions (90, 100, 110 and 120 °C) were thus recovered under argon atmosphere and analyzed by ^{11}B MAS NMR (Figure 8). They are denoted CsHB[90], CsHB[100], CsHB[110], and CsHB[120] respectively. The spectra of the samples CsHB[90], CsHB[100] and CsHB[110] are comparable. There are two signals at about -30 and -14 ppm. The former one is ascribed to a species comparable to the anion $B_3H_8^-$ [24-26]. The latter is due to a BH_2$ environment [19,21]. There is also a broad signal of high intensity at positive chemical shift. It is ascribed to BN_3$, and BN_2$H environments suggesting a polyborazylene-like solid [20,21]. There is also a signal of small intensity, particularly visible for CsHB[100] at 2 ppm, which may be due to a BN_4$ environment of a cross-linked polymeric compound [22]. It forms within the temperature range 90-110 °C. This same signal disappears at higher temperatures, suggesting a low stability of this species and their further evolution at temperatures higher than 110 °C. With respect to the spectrum of CsHB[120], the signals suggest only two types of compounds: a B_3H_8-like species (-32 ppm) and a cross-linked polyborazylene-like solid (other signals at > -2 ppm). These results are consistent with the decomposition extents measured at isothermal conditions (Figure 6): decomposed CsHB tends to form solid residues consisting of polyborazylene-like and a stable species likely to be CsB_3H_8, via the involvement of polymeric species with BH_2 groups (i.e. polyaminoborane-like).
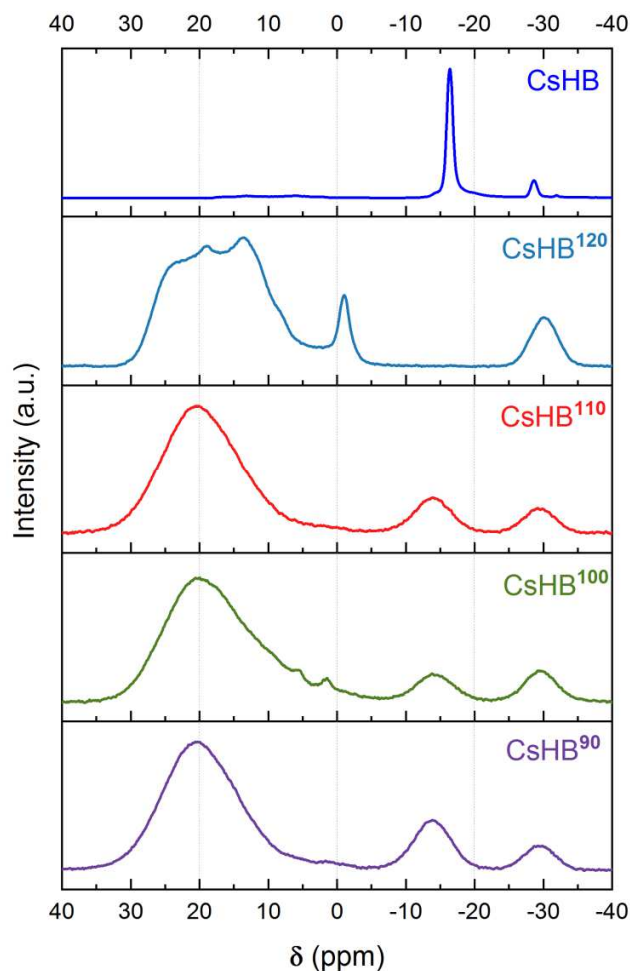
Figure 8. ^{11}B MAS NMR spectra of the solid residues recovered after the isothermal treatment at 90, 100, 110 and 120°C, namely CsHB^{90}, CsHB^{100}, CsHB^{110}, and CsHB^{120}. The spectrum of CsHB is given for comparison.

To mechanistically explain the improved dehydrogenation properties of MHB (versus the parent HB), it has been suggested the occurrence of the so-called metal cation driven hydride-transfer [15] where the key step is the in situ formation of the metal hydride M−H via H$^{\delta-}$ transfer from [N$_2$H$_3$BH$_3$]$^-$ to M$^+$:

$$MN_2H_3BH_3 \ (s) \rightarrow MH \cdots H-N_2H_2BH_2 \ (s) \tag{6}$$

Release of H$_2$ is initiated from the intermediate species MH···H−N$_2$H$_2$BH$_2$, such as:

$$MH \cdots H-N_2H_2BH_2 \ (s) \rightarrow MN_2H_2BH_2 \ (s) + H_2 \ (g) \tag{7}$$

18
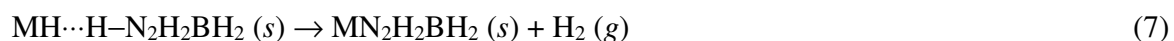
The further steps are intermolecular reactions of $MN_2H_2BH_2$ towards the formation of intermolecular N−B bonds leading to oligomeric/polymeric solids:

$$n\ MN_2H_2BH_2\ (s) \rightarrow [MBN_2H_{<2}]_n\ (s) + m\ H_2\ (g) \qquad (8)$$
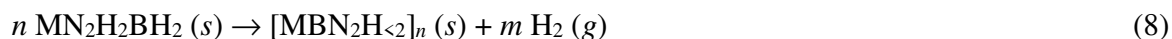
with $m > n$. Based on our observations, Cs^+ is not as efficient as e.g. Li^+ is for favoring the formation of pure H_2 according to the stepwise reactions mentioned above (Eqs. 6 to 8). And, Cs^+ cannot prevent the decomposition of $[N_2H_3BH_3]^-$ (Figure 7). In other words, CsHB in the form presented herein does not present suitable dehydrogenation properties to be considered as a potential hydrogen storage material. Further works are required to improve its properties and to better understand the formation of the unwanted CsB_3H_8, NH_3, B_2H_6, and N_2H_4.

4. Conclusion

The last of the alkali derivatives of hydrazine borane $N_2H_4BH_3$, cesium hydrazinidoborane $CsN_2H_3BH_3$ (CsHB; 3.3 wt. % H), was synthesized and characterized. The substitution of one $H^{\delta+}$ of the N_2H_4 moiety by Cs^+ has been demonstrated by FTIR and ^{11}B MAS NMR spectroscopy techniques. CsHB is a crystalline material. It is isostructural to $KN_2H_3BH_3$ and $RbN_2H_3BH_3$, with a monoclinic unit cell, a $P2_1$ space group (No. 4), and the following cell parameters: $a = 5.9156(5)$ Å, $b = 7.0091(5)$ Å, $c = 6.0023(5)$ Å, and $\beta = 108.389(4)°$. The thermal behavior of CsHB was studied. The destabilization effect of Cs^+ on the anionic entity $[N_2H_4BH_3]^-$ has been confirmed: (*i*) under heating at 5 °C min^{-1}, CsHB starts to decompose at a lower temperature than HB does; (*ii*) at isothermal conditions, e.g. at 120 °C, CsHB releases more equivalents of gas and more rapidly than HB, LiHB and RbHB do. However, CsHB decomposes rather than it dehydrogenates. Together with H_2, ammonia, hydrazine and diborane, for example, have been detected. In comparison to the other alkali hydrazinidoboranes, CsHB is definitely the least attractive in terms of H_2 purity. As for the parent hydrazine borane, the thermolytic solid residues forming upon decomposition of CsHB were found to be unstable (shock-sensitive and highly reactive towards O_2 and H_2O). This may be due to unidentified Cs-based and/or nitrogen-containing products. Otherwise, the ^{11}B MAS NMR analyses of the solid residues are indicative of the formation of polyborazylene-like products and possibly of CsB_3H_8.

By successfully synthesizing and studying cesium hydrazinidoborane, we have been able to complete the alkali family of the hydrazine borane derivatives. The present findings contribute to have a better knowledge of this kind of boron- and nitrogen-based materials. However, the thermal behavior of CsHB is not to its advantage: the released H_2 is polluted by several unwanted gaseous by-products and the thermolytic solid residue poses safety issues. CsHB in the form presented herein is thus not suitable for hydrogen storage. Otherwise, it might be considered as energetic material.

Acknowledgments

References

[1]   Dunn S. Hydrogen futures: Toward a sustainable energy system. Int J Hydrogen Energy 2002;27:235-64. https://doi.org/10.1016/S0360-3199(01)00131-8

[2]   Abe JO, Popoola API, Ajenifuja E, Popoola OM. Hydrogen energy, economy and storage: Review and recommendation. Int J Hydrogen Energy 2019;44:15072-86. https://doi.org/10.1016/j.ijhydene.2019.04.068

[3]   Barthelemy H, Weber M, Barbier F. Hydrogen storage: Recent improvements and industrial perspectives. Int J Hydrogen Energy 2017;42:7254-62. https://doi.org/10.1016/j.ijhydene.2016.03.178

[4]   Ren J, Musyoka NM, Langmi HW, Mathe M, Liao S. Current research trends and perspectives on materials-based hydrogen storage solutions: A critical review. Int J Hydrogen Energy 2017;42:289-311. https://doi.org/10.1016/j.ijhydene.2016.11.195

[5]   Kumar R, Karkamkar A, Bowden M, Autrey T. Solid-state hydrogen rich boron–nitrogen compounds for energy storage. Chem Soc Rev 2019;48:5350-80. https://doi.org/10.1039/C9CS00442D

[6]   Hügle T, Kühnel MF, Lentz D. Hydrazine borane: A promising hydrogen storage material. J Am Chem Soc 2009;131:7444-6. https://doi.org/10.1021/ja9013437

[7]   Moury R, Moussa G, Demirci UB, Hannauer J, Bernard S, Petit E, van der Lee A, Miele P. Hydrazine borane: Synthesis, characterization, and application prospects in chemical hydrogen storage. Phys Chem Chem Phys 2012;14:1768-77. https://doi.org/10.1039/C2CP23403C

[8]   Wu H, Zhou W, Pinkerton FE, Udovic TJ, Yildirim T, Rush JJ. Metal hydrazinoborane $LiN_2H_3BH_3$ and $LiN_2H_3BH_3 \cdot 2N_2H_4BH_3$: crystal structures and high-extent dehydrogenation. Energy Environ Sci 2012;5:7531-5. https://doi.org/10.1039/C2EE21508J

[9]   Moury R. Demirci UB, Ban V, Filinchuk Y, Ichikawa T, Zeng L, Goshome K, Miele P. Lithium hydrazinidoborane: A polymorphic material with potential for chemical hydrogen storage. Chem Mater 2014;26:3249-55. https://doi.org/10.1021/cm500980b

[10]   Moury R, Demirci UB, Ichikawa T, Filinchuk Y, Chiriac R, van der Lee A, Miele P. Sodium hydrazinidoborane: A chemical hydrogen-storage material. Chem Sus Chem 2013;6:667-73. https://doi.org/10.1002/cssc.201200800

[11] Chua YS, Pei Q, Ju X, Zhou W, Udovic TJ, Wu G, Xiong Z, Chen P, Wu H. Alkali metal hydride modification on hydrazine borane for improved dehydrogenation. J Phys Chem C 2014;118:11244-51. https://doi.org/10.1021/jp502144u

[12] Castilla-Martinez CA, Granier D, Charmette C, Maurin G, Yot PG, Demirci UB. Rubidium hydrazinidoborane: Synthesis, characterization and hydrogen release properties. Int J Hydrogen Energy 2019;44:28252-61. https://doi.org/10.1016/j.ijhydene.2019.09.064

[13] Favre-Nicolin V, Černý R. FOX, 'free objects for crystallography': A modular approach to ab initio structure determination from powder diffraction. J Appl Crystallogr 2002;35:734-43. https://doi.org/10.1107/S0021889802015236

[14] Petrícek V, Dušek M, Palatinus L. Crystallographic computing system JANA2006: General features. Z Kristallogr Cryst Mater 2014;229:345-52. https://doi.org/10.1515/zkri-2014-1737

[15] Kim DY, Lee HM, Seo J, Shin SK, Kim KS. Rules and trends of metal cation driven hydride-transfer mechanisms in metal amidoboranes. Phys Chem Chem Phys 2010;12:5446-53. https://doi.org/10.1039/B925235E

[16] Chua YS, Chen P, Wu G, Xiong Z. Development of amidoboranes for hydrogen storage. Chem Commun 2011;47:5116-29. https://doi.org/10.1039/C0CC05511E

[17] Wang K, Pan Z, Yu X. Metal B-N-H hydrogen-storage compound: Development and perspectives. J Alloys Compd 2019;794:303-24. https://doi.org/10.1016/j.jallcom.2019.04.240

[18] Hansen MR, Vosegaard T, Jakobsen HJ, Skibsted J. [11]B chemical shift anisotropies in borates from [11]B MAS, MQMAS, and single-crystal NMR spectroscopy. J Phys Chem A 2004;108:586-94. https://doi.org/10.1021/jp030939h

[19] Kim DP, Moon KT, Kho JG, Economy J, Gervais C, Babonneau F. Synthesis and characterization of poly(aminoborane) as a new boron nitride precursor. Polym Adv Technol 1999;10:702-12. https://doi.org/10.1002/(SICI)1099-1581(199912)10:12<702::AID-PAT931>3.0.CO;2-Q

[20] Gervais C, Maquet J, Babonneau F, Duriez C, Framery E, Vaultier M, Florian P, Massiot D. Chemically derived BN ceramics: Extensive ^{11}B and ^{15}N solid-state NMR study of a

preceramic polyborazylene. Chem Mater 2001;13:1700-7. https://doi.org/10.1021/cm001244l

[21] Stowe AC, Shaw WJ, Linehan JC, Schmid B, Autrey T. In situ solid state ^{11}B MAS-NMR studies of the thermal decomposition of ammonia borane: Mechanistic studies of the hydrogen release pathways from a solid state hydrogen storage material. Phys Chem Chem Phys 2007;9:1831-6. https://doi.org/10.1039/b617781f

[22] Kobayashi T, Gupta S, Caporini MA, Pecharsky VK, Pruski M. Mechanism of solid-state thermolysis of ammonia borane: A ^{15}N NMR study using fast magic-angle spinning and dynamic nuclear polarization. J Phys Chem C 2014;118:19548-55. https://doi.org/10.1021/jp504328x

[23] Shevlin SA, Kerkeni B, Guo ZX. Dehydrogenation mechanisms and thermodynamics of MNH_2BH_3 (M = Li, Na) metal amidoboranes as predicted from first principles. Phys Chem Chem Phys 2011;13:7649-59. https://doi.org/10.1039/C0CP02213F

[24] Hill TG, Godfroid RA, White JP, Shore SG. Reduction of $BH_3 \cdot THF$ by alkali metal (K, Rb, Cs) and ytterbium mercury amalgams to form salts of a simple procedure for the synthesis of tetraborane(10). Inorg Chem 1991;30:2952-4. https://doi.org/10.1021/ic00014a024

[25] Grinderslev JB, Møller KT, Yan T, Chen XM, Li Y, Li HW, Zhou W, Skibsted J, Chen X, Jensen TR. Potassium octahydridotriborate: Diverse polymorphism in a potential hydrogen storage material and potassium ion conductor. Dalton Trans 2019;48:8872-81. https://doi.org/10.1039/C9DT00742C

[26] Chen X, Ma N, Liu XR, Wei C, Cui CC, Cao BL, Guo Y, Wang LS, Gu Q, Chen X. Facile synthesis of unsolvated alkali metal octahydrotriborate salts MB_3H_8 (M = K, Rb, and Cs), mechanisms of formation, and the crystal structure of KB_3H_8. Angew Chem 2019;58:2720-4. https://doi.org/10.1002/anie.201812795

[27] Owarzany R, Jaroń T, Leszczyński PJ, Fijalkowski KJ, Grochala W. Amidoboranes of rubidium and caesium: The last missing members of the alkali metal amidoborane family. Dalton Trans 2017;46:16315-20. https://doi.org/10.1039/C7DT03590J

[28] Wu H, Zhou W, Yildirim T. Alkali and alkaline-earth metal amidoboranes: structure, crystal chemistry, and hydrogen storage properties. J Am Chem Soc 2008;130:14834-9. https://doi.org/10.1021/ja806243f

[29]   Chatterjee T, Thynell ST. Development of a reaction mechanism for liquid-phase decomposition of ammonia borane. Thermochim Acta 2019;682:178427. https://doi.org/10.1016/j.tca.2019.178427

[30]   Rizzi V, Polino D, Sicilia E, Russo N, Parrinello M. The onset of dehydrogenation in solid ammonia borane: an ab initio metadynamics study. Angew Chem Int Ed 2019;58:3976-80. https://doi.org/10.1002/anie.201900134

[31]   Shevlin SA, Kerkeni B, Guo ZX. Dehydrogenation mechanisms and thermodynamics of MNH_2BH_3 (M = Li, Na) metal amidoboranes as predicted from first principles. Phys Chem Chem Phys 2011;13:7649-59. https://doi.org/10.1039/C0CP02213F

[32]   Banu T, Sen K, Ash T, Das AK. Dehydrogenation of lithium hydrazinidoborane: Insight from computational analysis. Int J Hydrogen Energy 2016;41:18953-62. https://doi.org/10.1016/j.ijhydene.2016.08.218

$N_2H_4BH_3$

Cs

$CsN_2H_3BH_3$

H_2 Storage Material ?